Title
Light-Matter Interaction in Coupled Cavity Arrays with Disordered Emitters

Author
Chopra, Raunaq

Publication Date
2023

Light-Matter Interaction in Coupled Cavity Arrays with Disordered Emitters

By

RAUNAQ CHOPRA
THESIS

Submitted in partial satisfaction of the requirements for the degree of

Masters in Science

in

Electrical and Computer Engineering

in the

OFFICE OF GRADUATE STUDIES

of the

UNIVERSITY OF CALIFORNIA

DAVIS

Approved:

Marina Radulaski

Hussain al-Asaad

Richard T. Scalettar

Committee in Charge

2023

PREFACE

In this document, I present my master's thesis "Light-Emitter Interactions in Coupled Cavity Arrays with Disordered Emitters". This has been written to fulfill the graduation requirements of the Electrical and Computer Engineering Master's program at the University of California, Davis. I have been working on the research project and the writing of this thesis since November 2021.

While working towards my Bachelor's degree in Electrical and Computer Engineering, I noticed I seldom allowed myself the opportunity to step out of the comfort of my own subject. So, when I saw my supervisor, Dr. Marina Radulaski present research opportunities in her group, I noticed that this was an exciting opportunity to expand my horizons in a field that was largely unknown to me. Working on a research project outside of the realm of electrical engineering helped me gain a more wholesome experience in my Master's degree, while allowing a change of pace into a novel, challenging field. Along the way, I also found myself growing personally, into a stronger person while learning to overcome my own hurdles.

I would like to take a moment to thank my supervisor, Dr. Marina Radulaski, for her guidance and support throughout the process. I chose you as my advisor because I knew you would provide me with challenges that would help me grow, and am extremely grateful for that. I would also like to thank the team of researchers in your group for their thoughtful and encouraging insights. Also, many thanks to Professor Hussain Al-Asaad and Professor Richard Scalettar for being part of my journey towards obtaining a Master's degree.

Finally, and just as importantly, I want to thank my family and friends for being there for me. I would also like to thank you, my reader: I hope you enjoy your reading as much as I enjoyed writing.

Raunaq Chopra

University of California, Davis; March 13, 2023

ABSTRACT

The contents of this thesis examine the conditions under which the probability of light-matter interactions increases inside reflective cavities. Such interactions lead to the formation of a quasi-particle known as a polariton. Previous studies have explored, in detail, the conditions under which polaritons are formed when the matter (emitter) emits at the same frequency as the energy of the cavity (that is, when the system is resonant). This thesis explores the conditions of formation of polaritons when emitters across multiple cavities do not have the same energy (that is, emitters are disordered).

While such interactions have been studied with theoretical models thus far, it is likely that if polaritons are experimentally created in arrays of cavities, it will be with disordered emitters, for example in Silicon Carbide or diamond color center systems. To gain the most out of their applications, such as quantum simulators and quantum communication, it becomes prudent to study the conditions of their formation in a more realistic (disordered) setting. Since most prominent studies currently focus on resonant cases, they do not provide a complete picture about the behavior of experimentally created polaritons. In the research summarized in this dissertation, I discuss my findings about some differences between resonant and disordered systems.

Keywords: resonator, emitter, polariton, polaritonicity, eigenstates

CHAPTER 1

INTRODUCTION

1.1 What is Cavity Quantum Electrodynamics?

Since the nineteenth century, renowned physicists have studied the quantized nature of energy. Since then, it has become well known that excited electrons emit their energy as photons with discrete energy levels while returning to their ground state, and that the emitted light escapes to infinity.

In Cavity Quantum Electrodynamics (CQED), an atom is instead placed inside an optical resonator or a cavity. When its electrons return to the ground state and emit photons at certain frequencies, the photons get confined by the cavity and therefore lead to increased light-matter interactions [1]. In this thesis, I summarize my findings on such light-matter interactions inside resonator arrays or coupled cavity arrays.

1.1.1 Relevant terminology and symbols

As an aid for this thesis, a few relevant terms and their definitions have been included. These will be referred to throughout the dissertation.

Emitter: A two-level system containing excitable electrons, whose transitions from an excited state $|e\rangle$ to the ground state $|g\rangle$ results in emission of photons into the resonator, while the absorption of a photon leads to a transition from $|g\rangle$ to $|e\rangle$.

Optical Cavity: Also known as an optical resonator, an optical cavity resonates light at a specific frequency (such that the wavelength matches the size of the cavity), or at a set of specific frequencies.

Cavity-Emitter Coupling Constant: The rate of excitation exchange between the cavity and the emitter, symbolized by g [2]. Not to be confused with the ground state of an electron, $|g\rangle$.

Cavity Loss Rate: Rate of photons leaking out of the cavity due to finite reflectivity of the cavity, symbolized by κ [3]. This is a non-ideality because ideal resonators are lossless, that is, for ideal resonators, $\kappa = 0$.

Emitter Rate: Rate of spontaneous emission of photons from an emitter, symbolized by γ. This is a non-ideality because photons are emitted into free space instead of into the resonator, as seen in Figure 1.

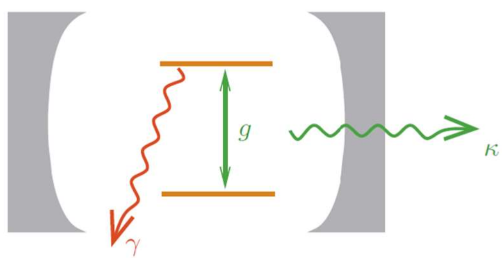

Figure 1: Pictorial representation of a resonator, showing some of the parameters discussed above. Image taken from Figure 1 of [4].

Strong and Weak Coupling Regime: A cavity-emitter pair with $g > \gamma/2$ and $g > \kappa/2$ is said to be in the strong coupling regime. Small values of κ and γ mean that the emitted photon has a greater probability of interacting, or coupling, with the emitter.

Polariton: A quasi-particle formed by superposition of light and matter.

Polaritonicity: Also known as the polaritonic participation ratio, this quantity measures the degree of light-matter hybridization of the wavefunction. This quantity is normalized between 0 and 1, where 0 represents completely emitter-like or cavity-like behavior, while 1 represents an equal superposition of cavity and emitter components. Polaritonicity can attain any intermediate value. Mathematically, polaritonicity can be defined as follows [5]:

$$P_P = \left[\left(\sum_{n=1}^{N} \langle \mathcal{N}_{ph,n} \rangle \right)^2 + \left(\sum_{n=1}^{N} \langle \mathcal{N}_{e,n} \rangle \right)^2 \right]^{-1} \tag{1}$$

Here, $\mathcal{N}_{ph,n} = a_n^\dagger a_n$ and $\mathcal{N}_{e,n} = \sigma_n^+ \sigma_n^-$ (please see chapter 2 for further details).

Nodal Participation Ratio: A measure for the localization of the photon wavefunction. Localization prevents photons from moving from one cavity to another in a coupled-cavity system.

Cavity Occupancy: The probability of the cavity being occupied by a photon, an excitation, or a polariton.

Hamiltonian: An operator that specifies the total energy of the system. The Hamiltonian acts on the wavefunction of the system to represent all possible energy transitions over time. The eigenvalues of the Hamiltonian represent the possible energy values in a quantized system. The corresponding eigenvectors represent the wavefunctions which, in cavity QED, reveal whether a state is polaritonic or localized.

Hopping Rate: Defined for a multi-cavity system, the hopping rate is the rate at which photons move from one coupled cavity to another. Symbolized by J.

1.2 Aim of the Model

As mentioned above, polaritons are formed when the cavity mode (photon) and the emitter excitation both contribute to the wavefunction of the system. However, for this coupling to occur, several factors must work in harmony. In this model, we alter several parameters and observe the conditions that lead to the most polaritonic state in a set of resonators.

Previous models have provided detailed descriptions of cavity-emitter behavior for resonant emitters-cavity pairs. However, literature in the field of cavity QED has seldom explored the effects of disorder (resonance and disorder are described in chapter 2). In this model, we use previous research as a baseline to compare the effects of disorder against.

1.3 Methodology

The model in consideration is a theoretical model. Therefore, it is intuitive to use a computer based simulation to explore this model and its implications. Therefore, the study on this model is conducted using Python. Using programming allows several advantages over a physical experiment. The biggest advantage for a theoretical model such as the one described below, is the amount of control we have over different parameters. We can simulate ideal (resonant) conditions, and use these conditions as a baseline to compare against any disorder. Further, we can manipulate individual parameters and explore their effect without perturbing other values in the simulation.

CHAPTER 2

LITERATURE REVIEW AND THEORY

This section covers the theoretical concepts behind cavity quantum electrodynamics.

2.1 A Review of Light-Matter Interactions

Early research in quantum physics revealed the discrete nature of energy levels in atomic orbitals. It was found that, when an electron moves from various levels of excited states to its ground state, the emitted light consists of a set of discontinuous wavelengths, resulting in unique spectral patterns for atoms of different elements. Energy and wavelength are related to each other as follows:

$$E = \frac{hc}{\lambda} \tag{2}$$

Since the emitted light consists of discontinuous wavelengths, it can be concluded that there are only certain discrete energy levels between which electrons move, as shown in Figure 2:

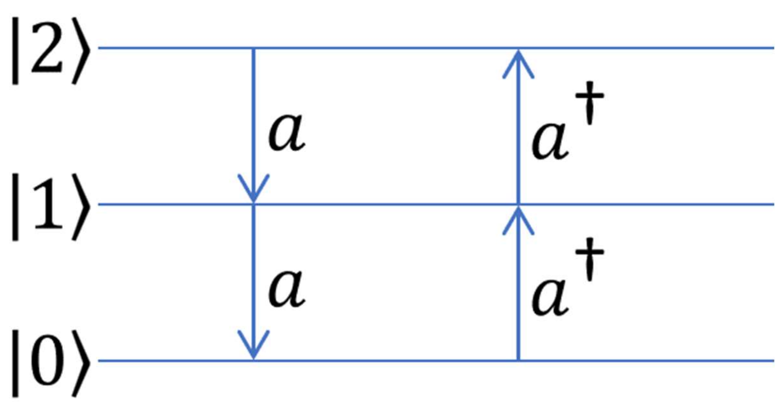

Figure 2: Excitations are created or destroyed as electrons move up or down energy levels.

Movement along these energy levels causes the creation or destruction of excited states. Excitation is shown with a symbol $a^{\dagger}$ (the creation operator, for the creation of an excited state), and a transition towards lower energy states is symbolized with a (the annihilation operator). Creation and annihilation operators are matrix operators such that $a^\dagger = \mathrm{adj}(a)$. The mathematical application of these operators on an energy state $|n\rangle$ is shown in expressions (3) and (4):

$$a^\dagger|n\rangle = \sqrt{n+1}\,|n+1\rangle \tag{3}$$

$$a|n\rangle = \sqrt{n}\,|n-1\rangle \tag{4}$$

When the creation operator is applied to state $|n\rangle$, an electron in this state rises to $|n+1\rangle$. Similarly, assuming $|n\rangle$ is an excited state, then the annihilation operator shows the movement of an electron to the next lower state, $|n-1\rangle$. The square root terms in expressions (3) and (4) appear because of the definition of $a^\dagger$ and a; the details of the origin of these terms are omitted [6].

A more general matrix operator, called a Hamiltonian $(\mathcal{H})$, determines the total energy evolution of a system over time [7]. The creation and annihilation operators are often used in deriving Hamiltonian operators. The details of Hamiltonians are covered in the next few sections.

2.2 Application to a Resonator

If a photon is introduced to a resonator containing an emitter, one of two events might occur. If the photon's energy is too low, it will fail to excite an electron even if the photon tries to interact with the atom. Otherwise, in a case where the photon's energy is high enough, then an electron will enter an unstable excited state upon interaction with the photon [8].

Since the excited state is not stable, the electron will spontaneously return to the ground state, once again emitting a photon with energy equal to the energy lost by the electron. Reflection and re-absorption of this photon causes the emitter to transition to the excited state again. This process repeats itself rapidly enough that to an external observer, the photon and the excited emitter appear as a superimposed state called a polariton.

2.3 The Frequency of the Photons

From the preceding discussion, one important detail is yet to be addressed: the frequency of the light. In this model, there are two relevant frequencies: the center frequency and the emitter frequency.

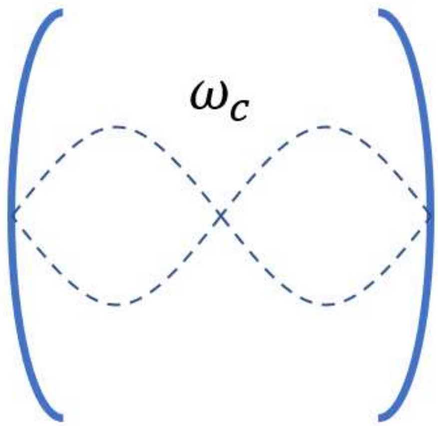

Figure 3: The center frequency has a corresponding wavelength that equals the width of the cavity.

The center frequency, symbolized as ω_c, has a corresponding wavelength that is equal to the width of the cavity, as shown in Figure 3. The emitter frequency, symbolized as ω_e, is the frequency of the light emitted by the emitter in a transition from $|e\rangle$ to $|g\rangle$. A cavity-emitter pair is resonant when $\omega_c = \omega_e$.

If the center frequency and emitter frequency are not equal, the system is said to be off-resonant. In multi-emitter systems, emitters might have different frequencies from one another. Such systems are said to be spectrally disordered.

In subsequent sections, we will observe the impacts of disorder on polaritonicity, and how disordered systems differ from resonant systems.

2.4 Models of Resonator-Emitter Interactions

This thesis is focused on a model called the Jaynes-Cummings-Hubbard (JCH) Model. This model consists of multiple coupled resonators organized in a linear array [as seen in Figure 4(c)], each with a single emitter. To derive the Hamiltonian for this model, we first derive the Hamiltonian of its elements. We will derive the JCH Hamiltonian in section 2.4.5 using results from preceding sections.

2.4.1 The Resonator

The operators $a^\dagger$ and a increase or decrease the number of excitations in a resonator. The energy corresponding with an excitation in a resonator is given by $\hbar\omega_c$, so the Hamiltonian for a resonator can be written as follows:

$$\mathcal{H}_R = \hbar\omega_c a^\dagger a \tag{5}$$

It may be prudent to point out here that using expressions (3) and (4), applying the $a^\dagger a$ operation to a state $|n\rangle$ returns $n|n\rangle$. In this case, n can be used to represent the number of photons present in the resonator.

2.4.2 The Emitter

Unlike the resonator, emitters consist of only two energy levels: a ground state and a single excited state. So, a different set of operators is defined: the raising (σ^+) and lowering (σ^-) operators replace creation and annihilation operators. When acting on a ground state, the raising operator causes a transition to the excited state:

$$\sigma^+|g\rangle = |e\rangle \tag{6}$$

Similarly, when the lowering operator acts on an excited state, then we observe a transition to the ground state:

$$\sigma^{-}|e\rangle = |g\rangle \tag{7}$$

Since the emitter has only two states, $\sigma^{+}|e\rangle$ and $\sigma^{-}|g\rangle$ operations are not allowed because there is no vacant state above the excited state, and no vacant state below the ground state.

The Hamiltonian corresponding with the emitter is thus defined as follows:

$$\mathcal{H}_E = \hbar\omega_e\sigma^{+}\sigma^{-} \tag{8}$$

It can be observed that the emitter Hamiltonian is like the resonator Hamiltonian. First, there is an energy term $\hbar\omega_e$ to measure the amount of energy that is transferred in a transition. Then, the raising and lowering operators represent transitions that occur with this amount of energy.

2.4.3 The Jaynes-Cummings Hamiltonian

The Jaynes-Cummings model is the simplest resonator-emitter model. This model consists of a single emitter in a single cavity, as shown in Figure 4(a). The Hamiltonian for this term consists of three parts:

- A resonator component, whose Hamiltonian is given by expression (5)
- An emitter component, whose Hamiltonian is given by expression (8)
- A superposition of the resonator and the emitter. As previously defined, the transition between $|e\rangle$ and $|g\rangle$ has a probability g. Further, a transition can be characterized in one of two ways: the creation of an excitation of the resonator (photon generation) and the lowering of an electron $(a^{\dagger}\sigma^{-})$, or the annihilation of the excited state and raising of an electron $(a\sigma^{+})$

Accounting for these three parts, the Jaynes-Cummings Hamiltonian can be written as:

$$\mathcal{H}_{JC} = \hbar\omega_c a^{\dagger}a + \hbar\omega_e\sigma^{+}\sigma^{-} + \hbar g(a^{\dagger}\sigma^{-} + a\sigma^{+}) \tag{9}$$

In this expression, the first term represents the energy of the photons in the cavity. The second term represents the energy of the emitter excitation, while the third term represents the interaction of light with the emitter. Since the first two terms represent a resonator and an emitter component, these typically dominate in a system with low polaritonic participation ratio. On the other hand, the third term dominates when the system has high polaritonicity.

2.4.4 The Tavis-Cummings Hamiltonian

The Tavis-Cummings model consists of a single resonator with multiple emitters, as shown in Figure 4(b). Like the Jaynes-Cummings model, this Hamiltonian has three parts. Since this model still consists of a single resonator, the resonator term remains unchanged. However, for the emitter and the superposition, we must account for each emitter, as seen below:

$$\mathcal{H}_{TC} = \hbar\left[\omega_c a^\dagger a + \sum_{i=1}^{M} \omega_{ei}\sigma_i^+\sigma_i^- + \sum_{i=1}^{M} g_i(a^\dagger\sigma_i^- + a\sigma_i^+)\right] \tag{10}$$

In expression (10), M represents the number of emitters in the resonator.

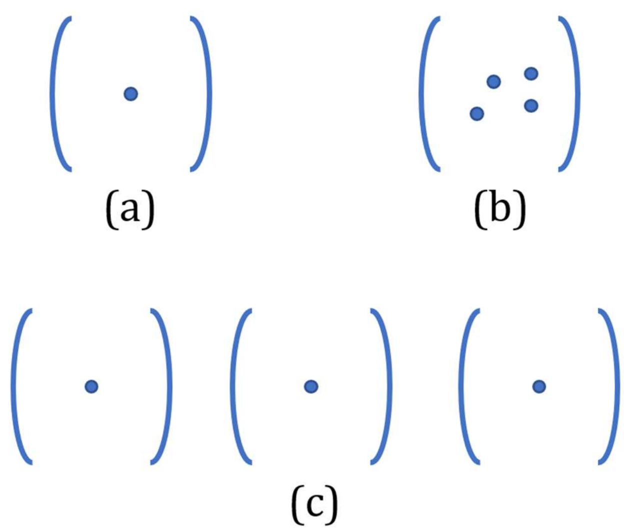

Figure 4: Schematic representation of (a) the Jaynes-Cummings Model, (b) the Tavis-Cummings Model and (c) the Jaynes-Cummings-Hubbard model.

2.4.5 The Jaynes-Cummings-Hubbard Hamiltonian

As mentioned previously, the Jaynes-Cummings-Hubbard model consists of multiple resonators, each with a single emitter, as shown in Figure 4(c). Here, the Hamiltonian must account for each resonator. Additionally, since each resonator contains one emitter, the emitter term will also consist of a summation.

Finally, the resonators are coupled with each other. This means that photons can hop from one resonator to the other. This is also considered in the Hamiltonian by including the final term. Note that in this term, we have an $a_i^\dagger a_{i+1}$ term to represent a photon hopping from $(i+1)^{st}$ to i^{th} cavity, and the $a_{i+1}^\dagger a_i$ term to represent a photon hopping from i^{th} to $(i+1)^{st}$ cavity. The resulting Hamiltonian for the JCH model is thus derived as [9]:

$$\mathcal{H}_{JCH} = \hbar \sum_{i=1}^{N} \left(\omega_{ci} a_i^\dagger a_i + \omega_{ei} \sigma_i^+ \sigma_i^- \right) + \hbar \sum_{i=1}^{N} g_i \left(a_i^\dagger \sigma_i^- + a_i \sigma_i^+ \right) - \hbar J \sum_{i=1}^{N-1} \left(a_i^\dagger a_{i+1} + a_{i+1}^\dagger a_i \right) \tag{11}$$

2.5 The Effective Hamiltonian Method

Evolution of closed quantum systems is described by the time-independent Schrödinger equation in the following form:

$$\mathcal{H}\psi = E\psi \tag{12}$$

However, in experiment, systems are affected by losses of cavities and emitters to the environment. To describe the full dynamics of such a system in a computationally efficient way, we resort to using an effective Hamiltonian of the form:

$$\mathcal{H}_{eff} = \mathcal{H}_{JCH} - i\hbar \sum_{j} \frac{\kappa}{2} a_j^\dagger a_j - i\hbar \sum_{j} \frac{\gamma}{2} \sigma_j^+ \sigma_j^- \tag{13}$$

This Hamiltonian is non-Hermitian (in contrast to the usual requirement of Hermitian Hamiltonians in quantum mechanics). This can be used to provide a satisfactory approximate solution only for the single excitation regime. However, this regime is experimentally relevant, and corresponds to optical control of the system with weak intensity.

2.6 The Eigenstates

In section 2.3, we demonstrated that ω_c corresponds with the frequency of an excited resonator, and that $\omega_e \approx \omega_c$ for a resonant system. However, when an emitter is coupled with a resonator, these energy levels split, as shown in Figure 5.

The energy of the newly formed levels can be calculated using the system's Hamiltonian. Equation (14) shows the Jaynes-Cummings Hamiltonian written in the matrix form; multiplying the matrices out returns expression (9):

$$\mathcal{H}_{JC} = \hbar\begin{pmatrix} a^\dagger & \sigma^+ \end{pmatrix} \underbrace{\begin{pmatrix} \omega_c & g \\ g & \omega_e \end{pmatrix}}_{h} \begin{pmatrix} a \\ \sigma^- \end{pmatrix} \tag{14}$$

Here, since we assume the system to be resonant, we set $\omega_e = \omega_c$. The eigenvalues of matrix h return the energies of the newly formed energy levels:

$$\begin{vmatrix} s-\omega_c & g \\ g & s-\omega_c \end{vmatrix} = 0$$

$$s = \omega_c \pm g \tag{15}$$

To obtain a more generalized perspective, we consider the Tavis-Cummings Hamiltonian with two emitters:

$$\mathcal{H}_{TC} = \hbar\begin{pmatrix} a^\dagger & \sigma_1^+ & \sigma_2^+ \end{pmatrix} \underbrace{\begin{pmatrix} \omega_c & g_1 & g_2 \\ g_1 & \omega_{e1} & 0 \\ g_2 & 0 & \omega_{e2} \end{pmatrix}}_{h} \begin{pmatrix} a \\ \sigma_1^- \\ \sigma_2^- \end{pmatrix} \tag{16}$$

If we assume $\omega_c = \omega_{e1} = \omega_{e2}$ and $g_1 = g_2 = g$ for resonant systems, and find the energy of the newly formed energy levels using the eigenvalues of h:

$$\begin{vmatrix} s-\omega_c & g & g \\ g & s-\omega_c & 0 \\ g & 0 & s-\omega_c \end{vmatrix} = 0 \tag{17}$$

Upon calculating the eigenvalues of expression (15), we will find an eigenvalue at $\hbar\omega_c$, and two more at $\hbar(\omega_c \pm g\sqrt{2})$. In general, for an M emitter system, we find an eigenvalue each at $\hbar(\omega_c \pm g\sqrt{M})$, and the rest of the eigenvalues are at $\hbar\omega_c$. For a single emitter then, we can obtain the energy levels by using $M = 1$, and we will obtain the same results as expression (15).

Typically, the offset of the split energy levels is negligible compared to the value of ω_c itself ($\omega_c \gg g\sqrt{M}$). For convenience, we use $\hbar\omega_c$ as the zero reference, and all other energy levels are represented relative to this value.

The two split energies each represent an eigenstate for a single resonator. So, for a JCH Model with N resonators, we obtain a total of $2N$ eigenstates.

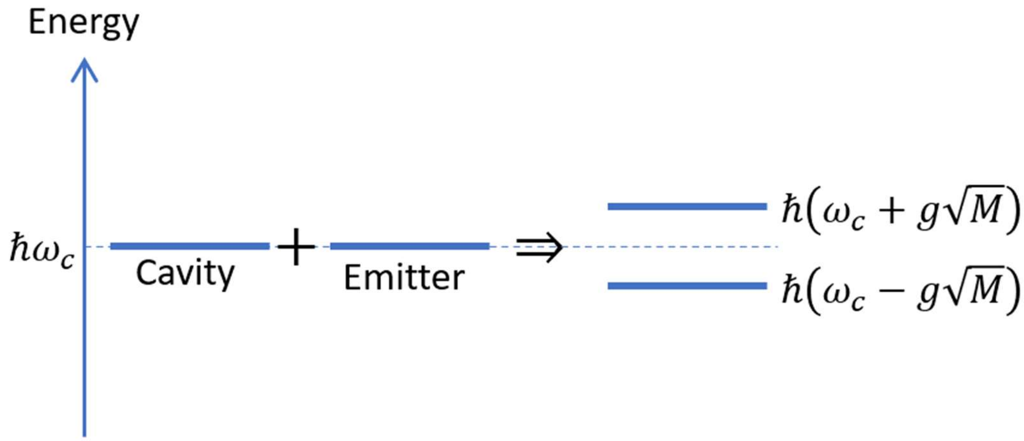

Figure 5: Energy splitting in a resonator with an emitter. Here, M is the number of emitters in the resonator (in the Jaynes-Cummings-Hubbard model, $M = 1$).

It is important to note that this solution does not account for cavity and emitter losses. Hence, we resort to analyzing the system using the Effective Hamiltonian approach described in section 2.5.

A more common representation of the energy splitting is shown in Figure 6. Here, the y axis gives the transmission rate of different frequencies if a laser is incident on a resonator coupled to an emitter. In Figure 6(a), we observe the transmission rate of a lossless system, whereas Figure 6(b) represents a system with κ and γ losses.

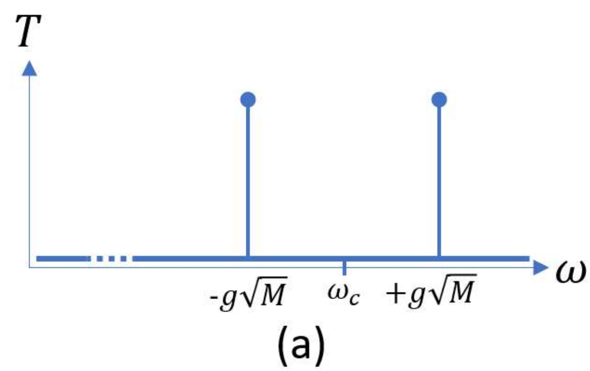

Figure 6: Transmission as a function of frequency. The two peaks occur because an emitter is present in the resonator, representing a polaritonic state in a (a) lossless system and (b) in a lossy system.

The splitting of energy necessitates the presence of an emitter in the cavity. Since an emitter is inserted to an excited resonator, the presence of two peaks in Figure 6 represent the presence of a polaritonic state.

In Chapter 3, we will consider several conditions for the JCH model, and explore situations that lead to a high likelihood of forming polaritonic states.

CHAPTER 3

THE MODEL AND THE RESULTS

This chapter briefly discusses the setup of the model, the results, and its implications. We take into consideration three cases, each of which is discussed below.

3.1 A Jaynes-Cummings-Hubbard Model with $N = 5$ Resonators, no Disorder

The initial dataset consists of five resonators, each with one emitter. The following values are used for some necessary quantities:

Quantity	Value used
Cavity-Emitter Coupling Constant, g	20 GHz
Cavity Loss Rate, κ	15 GHz
Emitter Loss Rate, γ	${}^{1}/_{5.8}$ GHz
Cavity Hopping rate, J	2 GHz and 200 GHz; both values simulated and their results compared

Table 1: Values of some frequently used quantities. These are typical values obtained from [10, 11, 12].

The values of g, κ and γ put the system in the strong coupling regime. Since $M = 1$ for the JCH Model, the energy of each eigenstate is expected to be around $\omega_c \pm g\sqrt{M} = \omega_c \pm 20$.

By applying the principles derived in section 2.6, we can represent the JCH Hamiltonian as a matrix, shown in expression (18).

$$\mathcal{H}_{JCH} = \hbar\begin{pmatrix} a_1^\dagger & a_2^\dagger & a_3^\dagger & a_4^\dagger & a_5^\dagger & \sigma_1^+ & \sigma_2^+ & \sigma_3^+ & \sigma_4^+ & \sigma_5^+ \end{pmatrix} h \begin{pmatrix} a_1 \\ a_2 \\ a_3 \\ a_4 \\ a_5 \\ \sigma_1^- \\ \sigma_2^- \\ \sigma_3^- \\ \sigma_4^- \\ \sigma_5^- \end{pmatrix} \tag{18}$$

In this case, the matrix h is represented as follows:

$$h = \begin{pmatrix} \omega_c & J & 0 & 0 & 0 & \vdots & g & 0 & 0 & 0 & 0 \\ J & \omega_c & J & 0 & 0 & \vdots & 0 & g & 0 & 0 & 0 \\ 0 & J & \omega_c & J & 0 & \vdots & 0 & 0 & g & 0 & 0 \\ 0 & 0 & J & \omega_c & J & \vdots & 0 & 0 & 0 & g & 0 \\ 0 & 0 & 0 & J & \omega_c & \vdots & 0 & 0 & 0 & 0 & g \\ \cdots & \cdots & \cdots & \cdots & \cdots & \vdots & \cdots & \cdots & \cdots & \cdots & \cdots \\ g & 0 & 0 & 0 & 0 & \vdots & 0 & 0 & 0 & 0 & 0 \\ 0 & g & 0 & 0 & 0 & \vdots & 0 & 0 & 0 & 0 & 0 \\ 0 & 0 & g & 0 & 0 & \vdots & 0 & 0 & 0 & 0 & 0 \\ 0 & 0 & 0 & g & 0 & \vdots & 0 & 0 & 0 & 0 & 0 \\ 0 & 0 & 0 & 0 & g & \vdots & 0 & 0 & 0 & 0 & 0 \end{pmatrix} \tag{19}$$

The diagonalization of matrix h gives us an informed guess for the eigenstates of the system. However, similar to section 2.6, this solution does not account for the cavity and emitter loss, necessitating analysis using the Effective Hamiltonian technique from section 2.5.

A quantity of interest in this model is J/g. For a low J/g ratio, photons tend to remain in the resonator where they originated, whereas a high J/g ratio means photons move from one cavity to another often. A high rate of photon movement means that photons get fewer opportunities to interact with emitters, thereby reducing the polaritonicity, as demonstrated in Figures 7 and 8.

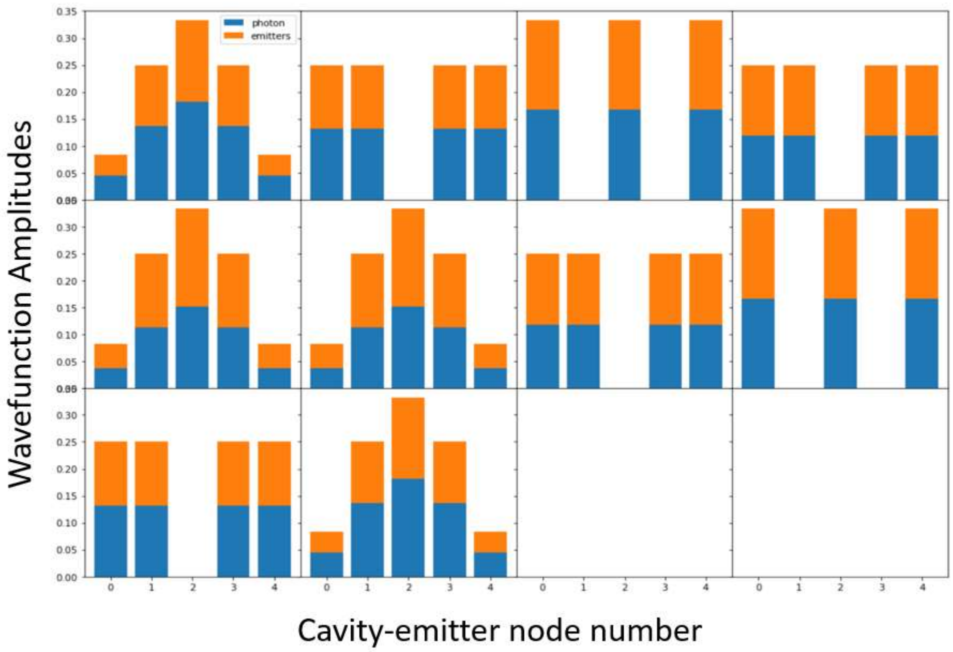

(a)

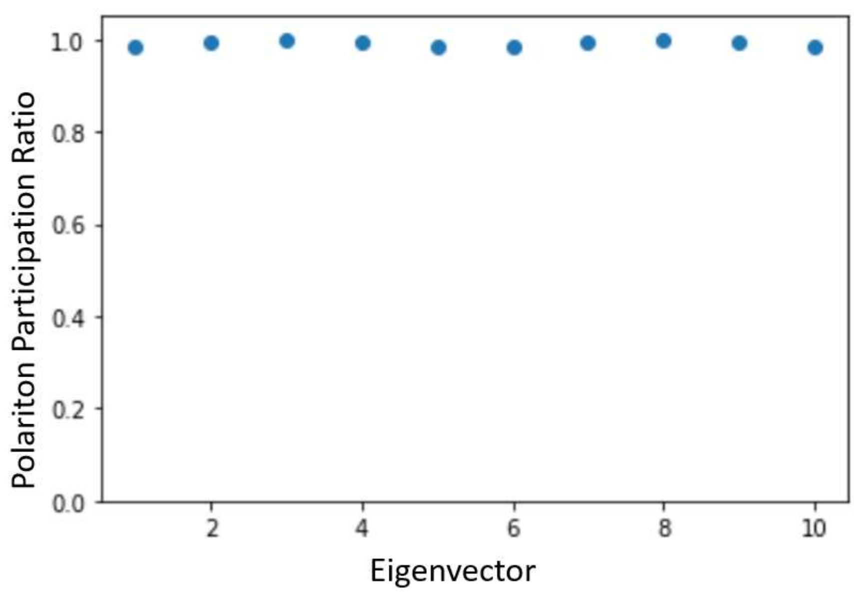

(b)

Figure 7: (a) Cavity occupancy for a N = 5 cavity system with J = 2GHz for each eigenvector. The blue bars represent the probability of finding a photon; the orange bars show the probability of finding an emitter excitation in the cavity. Bars with equal part blue and orange represent a polaritonic system. (b) The corresponding polaritonic participation ratio value for each eigenvector.

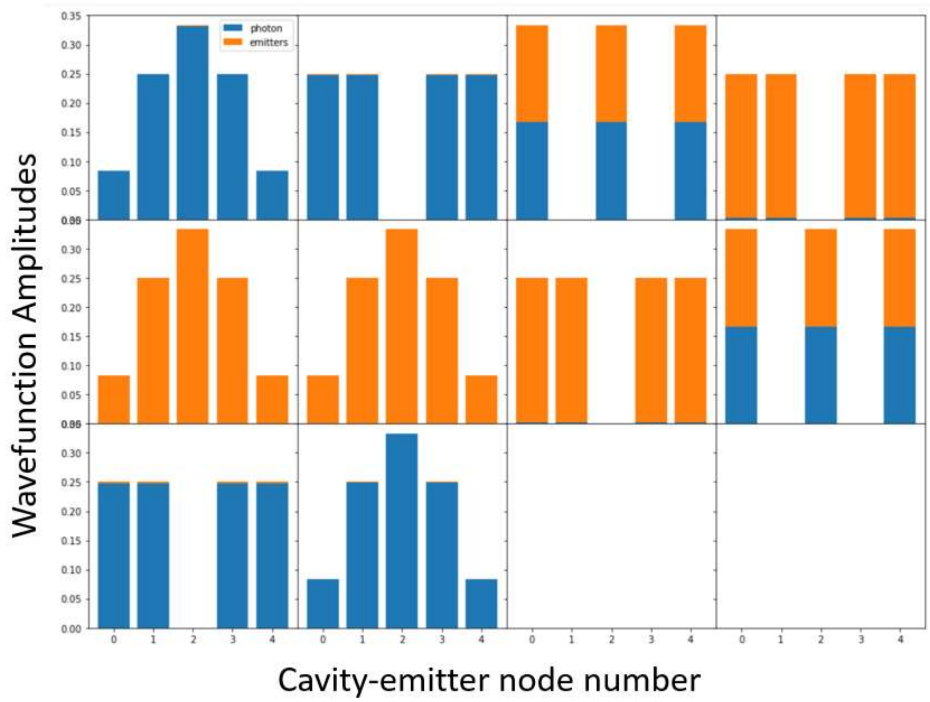

(a)

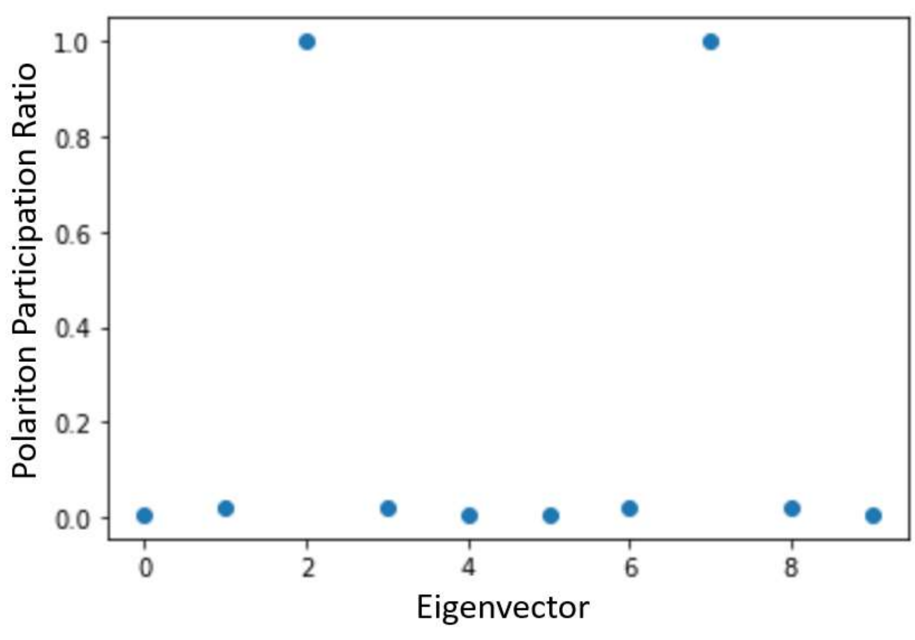

(b)

Figure 8: (a) Cavity occupancy for a N = 5 cavity system with J = 200GHz for each eigenvector. (b) The corresponding polaritonic participation ratio value for each eigenvector.

Figure 9 shows the corresponding energy plots for the two cases above. In Figure 9(a), with $J = 2$ GHz, we observe that all eigenstates have a frequency $\omega_c \pm 20$ GHz. This is as expected for a case with all polaritonic states.

In Figure 9(b), on the other hand, we note that the middle 4 eigenstates have $E \approx \hbar\omega_c$. This corresponds with a zero probability of finding a photon [as observed in Figure 8(a)], and these are called subradiant states. For an N resonator JCH model, there are $N - 1$ subradiant states between the two polaritonic states.

On the other end of the spectrum, the energy deviation of the first two and last two eigenstates is much larger than $g\sqrt{M}$. These states are also not polaritonic; instead, they exhibit completely photonic behavior and cannot interact with the emitters. There are only two eigenstates in between (the third and eighth eigenstate) whose frequency equals $\omega_c \pm g\sqrt{M}$. As seen in Figure 8, these eigenstates correspond to the most polaritonic states for a high J/g system.

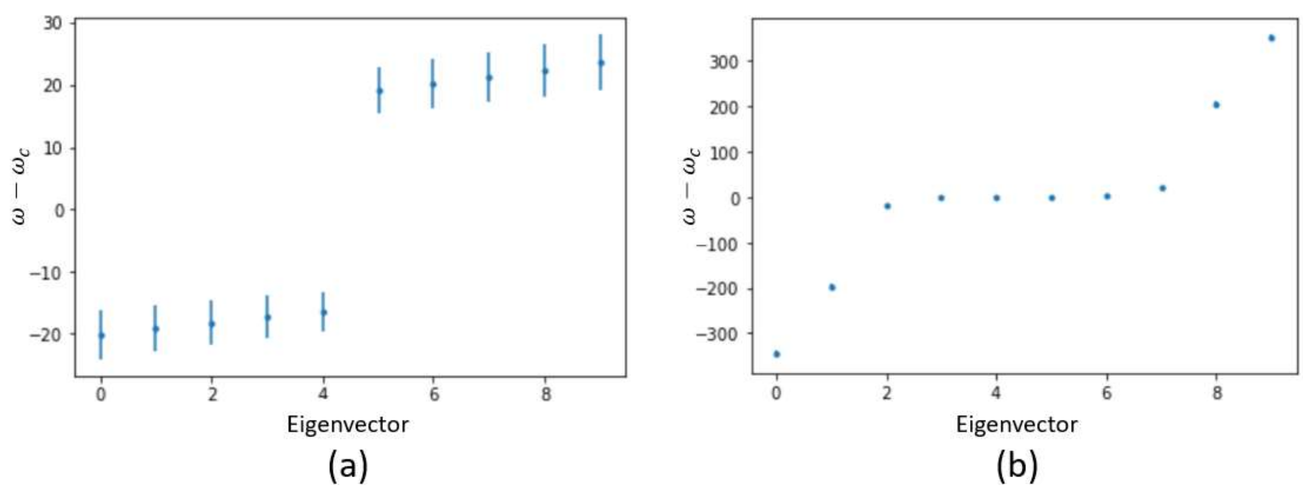

Figure 9: Energies of different eigenstates for (a) J = 2GHz and (b) J = 200GHz. Note that the 0 on the energy axis corresponds to $\omega - \omega_c = 0$.

3.2 The Disordered Jaynes-Cummings-Hubbard Model with $N = 5$ Resonators

In this subsection, we briefly explore the effects of disorder. As discussed in Chapter 2, a disordered system is one where emitters have different frequencies from one another. To simulate a disordered system, we introduce a random variable in a certain range, and add it to the emitter frequencies. In this case, we set the disorder to g. Figure 10 shows the energy vs. eigenvector plot for $J = 2$ GHz.

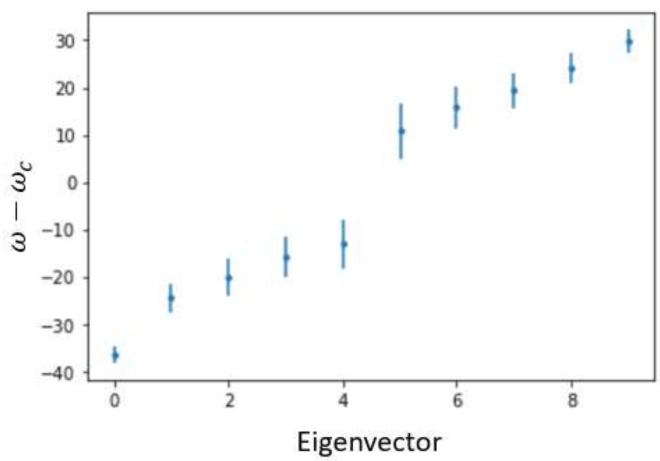

Figure 10: Energy vs. eigenvectors for a disordered system. Note that the energy values deviate more significantly from $\omega - \omega_c = g = 20$GHz, unlike the resonant system in Figure 9(a).

While comparing Figure 10 to Figure 9(a), we observe that the energy of the eigenvectors has some variation around $\omega - \omega_c = 20$ GHz. This is expected to result in a lower polaritonicity for each eigenstate, as shown in Figure 11. Upon inspecting Figure 11(a), we also notice that the cavity occupancies are more localized. This occurs because disorder impacts only the emitter frequencies. In this case, since $J/g = 0.1$, the localizing term g dominates. However, as seen in Figure 12, a high value of J allows for greater delocalization by allowing photons to hop from one cavity to another more frequently.

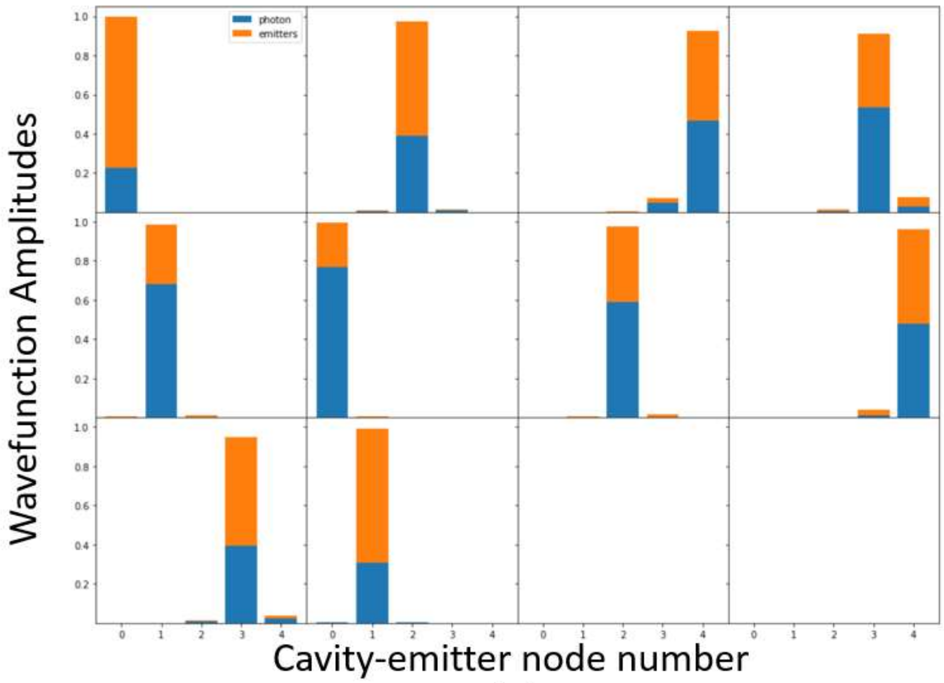

(a)

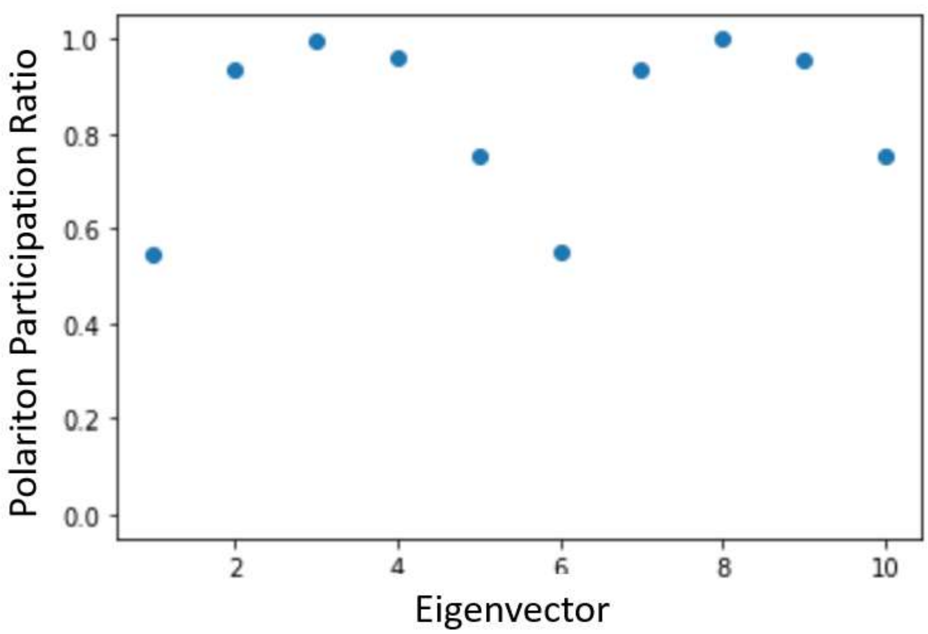

(b)

Figure 11: (a) Cavity occupancy for a $N = 5$ cavity system with $J = 2GHz$ for each eigenvector. (b) The corresponding polaritonic participation ratio value for each eigenvector.

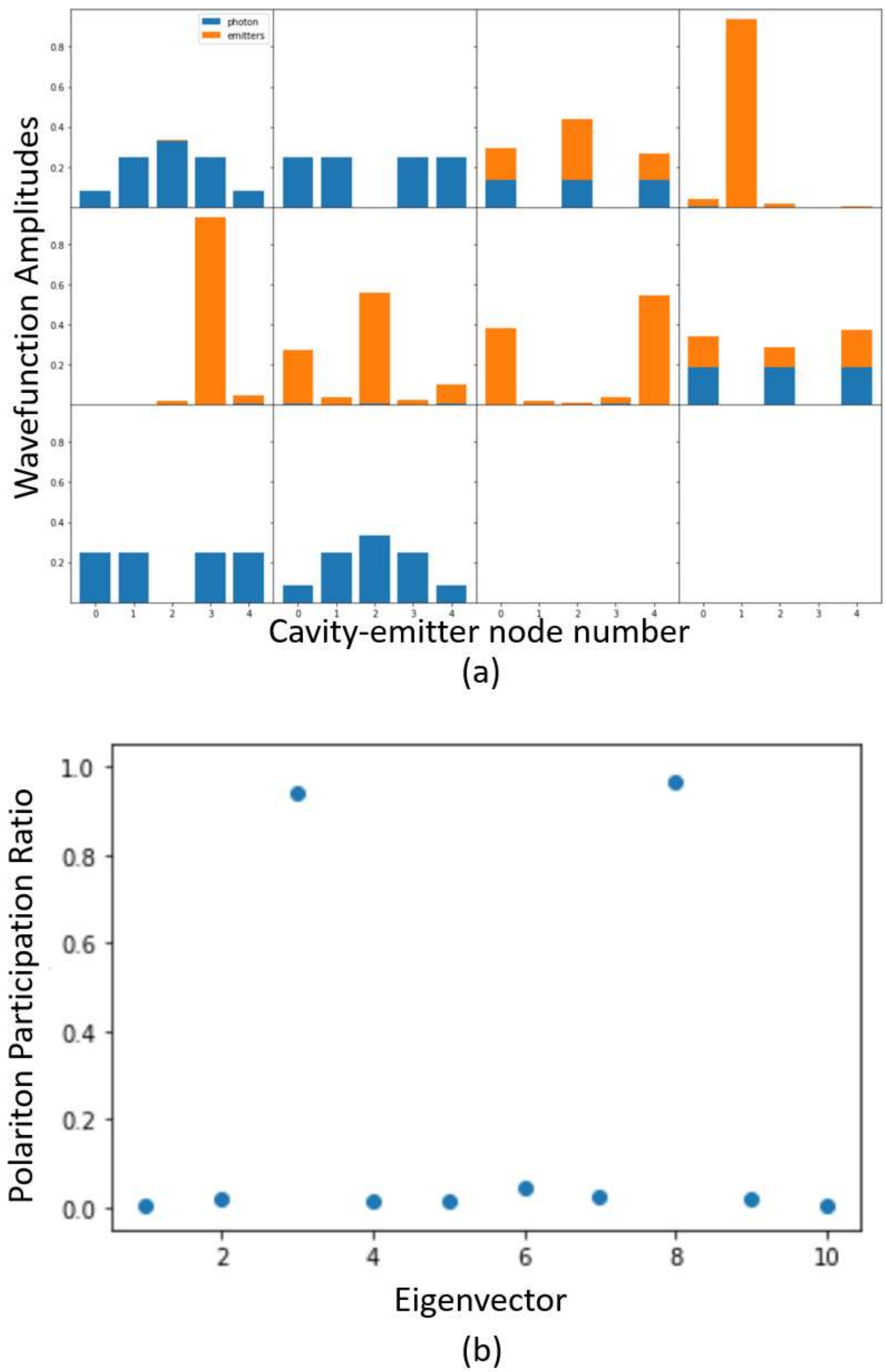

Figure 12: (a) Cavity occupancy for an N = 5 cavity system with J = 200GHz for each eigenvector. (b) The corresponding polaritonic participation ratio value for each eigenvector. Note that this system is relatively delocalized for most eigenstates and does not exhibit as much deviation from the resonant case as Figure 11 does.

To account for this difference in localization, we consider the nodal participation ratio. For a resonant system, such as the one in section 3.1, the resonators are delocalized, resulting in a high nodal participation ratio. On the other hand, a disordered system has a relatively lower nodal participation ratio. These results are captured in Figure 13.

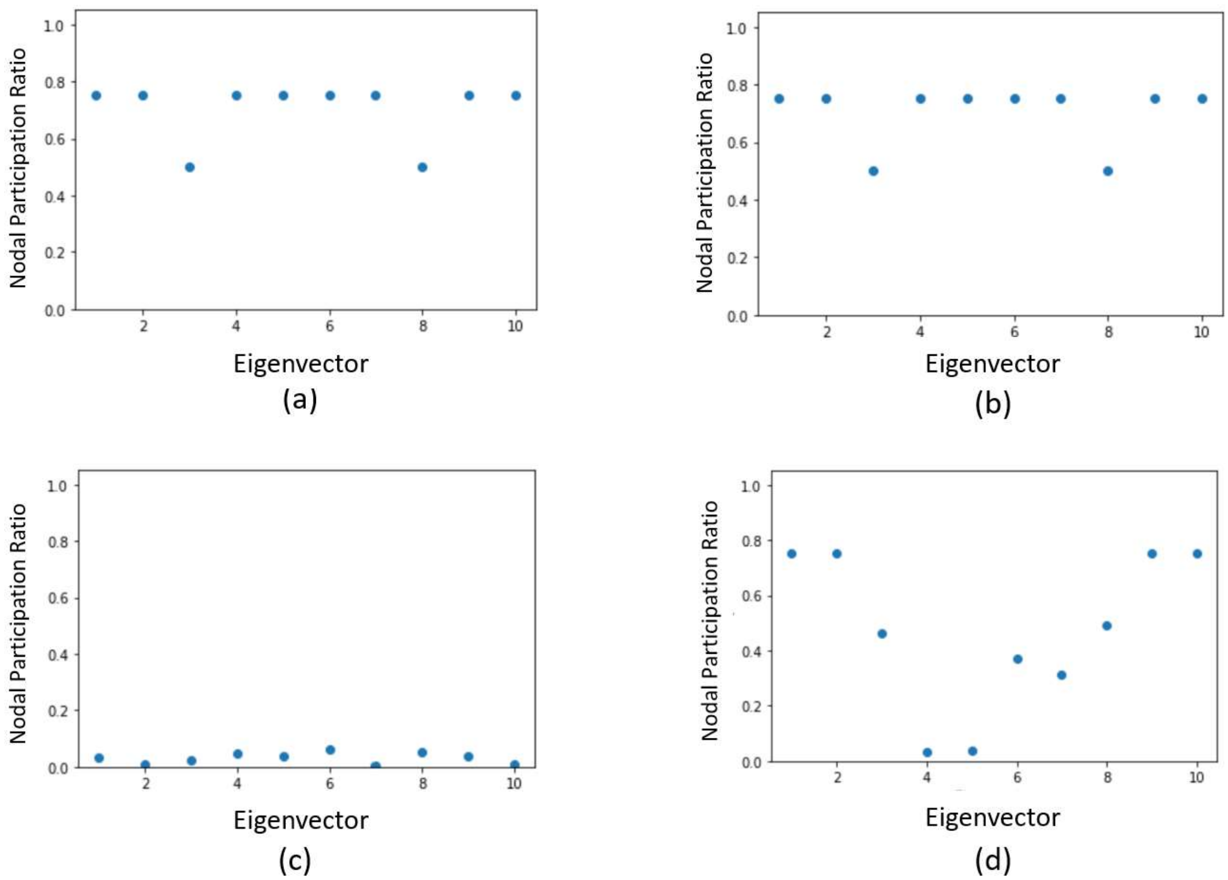

Figure 13: Nodal participation ratio without disorder for (a) $J = 2\text{GHz}$ and (b) $J = 200\text{GHz}$. Note that without disorder, the system looks delocalized for all J values. However, for disordered systems, (c) $J = 2\text{GHz}$ and (d) $J = 200\text{GHz}$ have different localization profiles as described above.

3.3 The Disordered Jaynes-Cummings-Hubbard Model with $N = 63$ Resonators

In the previous section, we considered single samples of disordered systems. While the sample provides useful insight, it does not provide a complete picture, as each simulation iteration yields unique results. To gain a better understanding, we now consider the average of 100 runs for a disordered system. The average of many runs presents a more comprehensive scenario, and the results are much more likely to repeat rather than being random, as was the case for section 3.2. In this section, we briefly explore a JCH model with 63 resonators, and a disorder of $0.25g$.

In addition, we redefine the cavity frequency in this section as follows [5]:

$$\omega_c = \omega_{c0} + 2J \cos k_t \tag{20}$$

Here, ω_{c0} is the cavity frequency which was being used previously. We referred to the value of ω_{c0} as 0 for simplicity.

One can argue that the previous sections used $k_t = \pi/2$ as this would lead to $\omega_c = \omega_{c0}$. These new values of ω_c lead to detuned systems. Since detuned systems have different center frequencies, the polaritonic eigenstates also change (this effect is more pronounced in highly delocalized systems).

For this section, we succinctly summarize our results in Figure 14. P_N represents the nodal participation ratio whereas P_P is the polaritonic participation ratio.

When $J/g = 0.1$, the system sees a low hopping rate, and therefore, high localization (as shown with consistently low P_N). Meanwhile, cavities are highly polaritonic, like the observation in the previous two sections.

As J increases, we expect the polaritonic states to be concentrated around a single value of k. Meanwhile, since photons can hop from one cavity to another, we expect greater delocalization, which is observed with higher P_N in Figure 14.

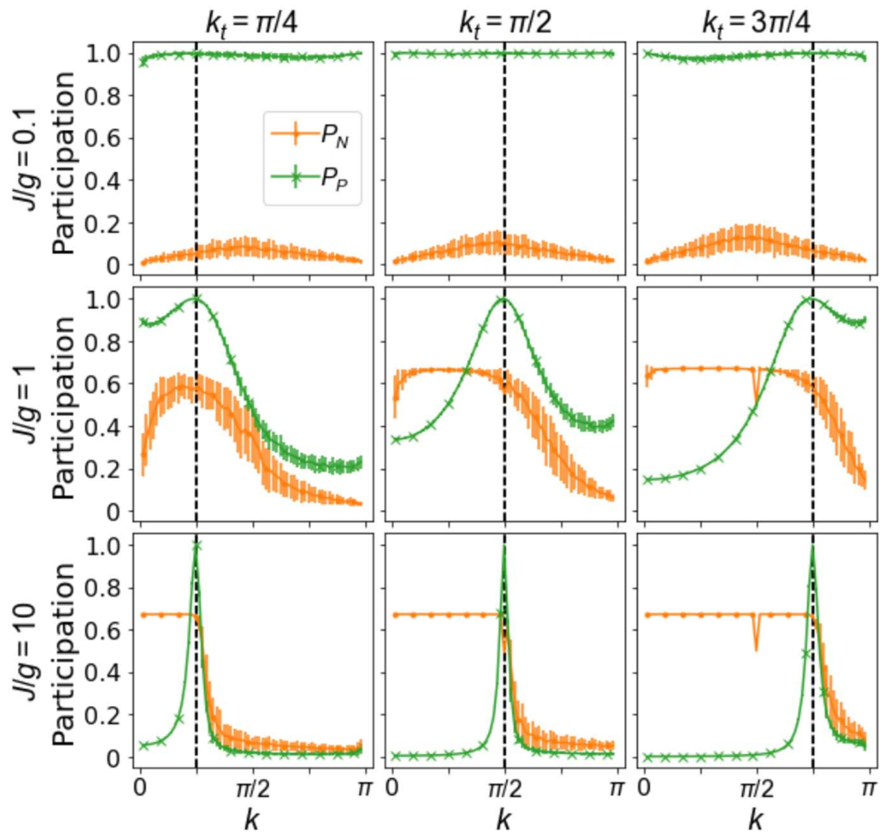

Figure 14: Polaritonic and Nodal Participation ratios for different hopping rates and detuning values for a system where disorder results in $\omega_e = \omega_{e0} \pm 0.25g$, where ω_{e0} is the emitter frequency before introducing disorder

An important observation is to be made here. For sections 3.1 and 3.2, where $k_t = \pi/2$, the most polaritonic state occurred in the middle of all the positive (or negative eigenstates), as shown in Figure 15. The peak for polaritonicity in Figure 14 represents this effect. Therefore, when the peaks are moved to the left or right, so are the most polaritonic states. This method leads to the creation of a tuning mechanism to engineer polaritonicity of wavefunctions in coupled cavity arrays.

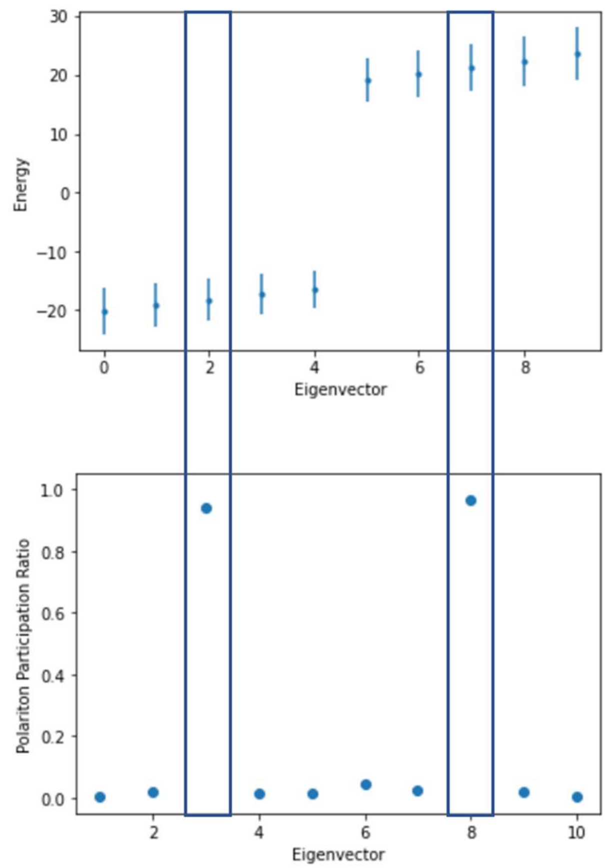

Figure 15: For $k_t = \pi/2$, the most polaritonic states are in the middle of the positive (and negative) energy eigenstates. By shifting k_t between 0 and π, we can shift the position of the most polaritonic state.

CHAPTER 4

CONCLUSION

4.1 Interpretation of Results

In chapter 3, we observed the polaritonicity of resonant and disordered states. We can conclude that polaritonicity decreases with increased hopping rates as well as with disorder. Despite this, we can affirm that polaritonic states can be attained in the presence of disorder of the order of the light and matter interaction in the system. For low hopping rates, high polaritonicity is expected for most eigenstates, but we also observe highly localized resonators. Meanwhile, high hopping rates result in more delocalization, but only a few eigenstates with high polaritonicity.

4.2 Applications

Our discussion this far has been focused on obtaining high polaritonicity. In this section, we discuss the benefits of highly polaritonic systems.

4.2.1 Quantum Communication

Coupled cavity networks provide platforms for quantum communication and information processing. To be able to achieve these, the system must be capable of entanglement and transmission of quantum states between distant nodes. Since emitters have a long life span, they can be used as quantum memories. Meanwhile, photons can rapidly move information across long distances. So, emitter-photon quasiparticles are promising components of a quantum network architecture [13]. For this network to exist, it is crucial to understand the conditions behind the formation of polaritonic states, because these will lay the foundation for such networks.

4.2.2 All photonic quantum simulators

In the recent years, strong interactions between photons and emitters have often been studied. This opens the possibility of using light-matter systems as all-photonic quantum simulators for many-body physics [4]. An important advantage of coupled cavity arrays, such as the ones studied here, is that each cavity can be individually accessed. This gives great control over experimental setup and provides a great platform for studying quantum phenomena.

References

[1] A. Lahiri, "Cavity Quantum Electrodynamics," in *Basic Optics: Principles and Concepts*, Amsterdam, Elsevier, 2016, p. 870.

[2] S. Barak, "The QED Coupling Constant for an Electron to Emit or Absorb a Photon is Shown to be the Square Root of the Fine Structure Constant α," *HAL Open Science,* vol. 4, 2020.

[3] Educational Documentaries, "Quantum Optics || 01 Lecture 29 Cavity QED Introduction," YouTube, 3 May 2020. [Online]. Available: https://www.youtube.com/watch?v=SF0-IzAeKyc. [Accessed 1 March 2023].

[4] M. J. Hartmann, F. G. S. L. Brandão and M. B. Plenio, "Quantum Many-body Phenomena in Coupled Cavity Arrays," *Laser & Photonics Reviews,* vol. 2, no. 6, pp. 527-556, 2008.

[5] J. Patton, V. A. Norman, R. T. Scalettar and M. Radulaski, "All-Photonic Quantum Simulators with Spectrally Disordered Emitters," 2022.

[6] E. Fradkin, "Second Quantization," [Online]. Available: http://eduardo.physics.illinois.edu/phys561/non_relativistic_final.pdf. [Accessed 17 March 2023].

[7] R. Eisberg and R. Resnick, "One Electron Atoms," in *Quantum Physics of Atoms, Molecules, Solids, Nuclei and Particles*, John Wiley & Sons, Inc, 1985, p. 262.

[8] R. Harris, "The Photoelectric Effect," in *Modern Physics*, Pearson Education Limited, 2014, p. 8.

[9] G. Blatter and S. Schmidt, "Strong Coupling Theory for the Jaynes-Cummings-Hubbard Model," *Physical Review Letters,* vol. 103, no. 8, p. 086403, 2009.

[10] V. A. Norman, S. Majety, Z. Wang, W. H. Casey, N. Curro and M. Radulaski, "Novel Color Center Platforms Enabling Fundamental Scientific Discovery," *Infomat,* vol. 3, no. 8, pp. 869-890, 2020.

[11] R. E. Evans, M. K. Bhaskar, D. D. Sukachev, C. T. Nguyen, A. Sipahigil, M. J. Burek, B. Machielse, G. H. Zhang, A. S. Zibrov, E. Bielejec, H. Park, M. Loncar and M. D. Lukin, "Photon-mediated Interactions Between Quantum Emitters in a Diamond Nanocavity," *Science Magazine,* vol. 362, no. 6415, pp. 662-665, 2018.

[12] S. Majety, V. A. Norman, L. Li, M. Bell, P. Saha and M. Radualski, "Quantum Photonics in Triangular Cross-section Nanodevices in Silicon Carbide," *Journal of Physics: Photonics,* vol. 3, no. 3, 2021.

[13] G. M. A. Almeida, F. Ciccarello, T. J. G. Apollaro and A. M. C. Souza, "Quantum-state Transfer in Staggered Coupled-Cavity Arrays," *Physical Review A,* vol. 93, no. 032310, 2016.

[14] F. Neese, L. Lang and V. Chilkuri, "Effective Hamiltonians," in *Topology, Entanglement, and Strong Correlations Modeling and Simulations*, Jülich, Verlag des Forschungszentrum Jülich, 2020, pp. 4.1-4.10.